(Received 11 September 2023, Accepted 29 October 2023, Scheduled 20 November 2023)

A Hierarchical PHM Framework for Phased Array Radar Systems

Delanyo K. B. Kulevome[1,2], Hong Wang[1,2,*], Zian Zhao[1], and Xuegang Wang[1]

[1] School of Information and Communication Engineering
University of Electronic Science and Technology of China, Chengdu 611731, China
[2] Yangtze Delta Region Institute (Huzhou), University of Electronic Science and Technology of China, Huzhou 313001, China

ABSTRACT: Phased array radar (PAR) systems are critical for modern defense and surveillance applications, but their reliability and availability are affected by various factors, including physical and performance degradation. Furthermore, implementing prognostics and health management (PHM) framework for the whole radar system is challenging. To address these issues, this paper proposes an efficient solution by hierarchically implementing PHM frameworks in an active PAR (APAR) system. The proposed framework subsumes device-level, subsystem-level, and system-level health prediction models to enable comprehensive health monitoring and maintenance decision-making. This approach addresses the unique challenges involved in implementing PHM for the APAR system and facilitates the transition from traditional reactive maintenance practices to a predictive maintenance approach, thereby improving the overall system. Mathematical models that relate the radar's physical degradation to its performance deterioration are formulated, analyzed, and presented. Subsequently, a Bayesian long short-term memory (BayesLSTM) architecture is developed and integrated into the proposed framework for estimating the remaining useful life (RUL) of critical devices/subsystems. The effectiveness of the proposed deep learning-based prognostic framework is evaluated through simulations and experimental studies. The proposed hierarchical framework has the potential to be applied to other radar systems that require effective health monitoring strategy.

1. INTRODUCTION

Phased array radars (PARs) are becoming increasingly popular due to their high performance and flexibility [1]. They are essential for modern military and civilian applications, including air traffic control, weather monitoring, and surveillance. However, these systems are complex and sophisticated, consisting of multiple devices and subsystems [2] that are susceptible to failure or degradation over time [3]. Physical deterioration, such as corrosion, mechanical wear, and thermal stress, can lead to performance degradation, including reduced range, accuracy, and reliability. The inherent complexity and criticality of these systems necessitate the development of robust prognostics and health management (PHM) frameworks to ensure their optimal performance, reliability, and availability.

PHM focuses on monitoring, assessing, and predicting the health and performance of systems to enable timely maintenance, reduce downtime, and enhance operational efficiency [4]. It plays a vital role in a wide range of industries, including aerospace [5], construction [7], and automotive [6] industries. PHM aims to provide system operators with actionable information regarding the health condition of a system, enabling them to make informed choices about maintenance, repair, and replacement strategies. Intelligent algorithms leverage sensor data and historical records to detect anomalies, identify faults, and predict the remaining useful life (RUL) or end-of-life (EoL) of critical devices or components.

The various PHM implementation techniques are based on model-based methods [8], data-driven methods [9], or hybrid approaches. Model-based methods utilize physics-based models or system knowledge to simulate the system's behavior and detect deviations from expected performance. On the other hand, data-driven approaches leverage advanced analytics and machine learning (ML) algorithms to analyze large volumes of data and identify patterns and trends associated with system health.

While existing PHM frameworks for systems have demonstrated effectiveness, the complexity of PAR demands a tailored approach that addresses the unique challenges they present. However, developing PHM for PAR can present several challenges, summarized as follows:

- **Challenge 1: System Complexity and Heterogeneity** — APAR comprises numerous interconnected devices and subsystems, making them highly heterogeneous and complex. Each device may have its failure modes, degradation patterns, and interactions. Capturing this complexity and developing physics-based models to handle the system's heterogeneity pose significant challenges in developing effective model-driven PHM frameworks.

- **Challenge 2: Data Availability and Quality** — APAR system generates vast data, including sensor readings and operational records. However, since maintenance strategies are based on predefined schedules, the full potential of the data acquired from the various sources is not fully utilized. Also, infrequent failures and, consequently, limited

* Corresponding authors: Hong Wang (hongw@uestc.edu.cn).

failure data, pose challenges for developing data-driven predictive models.

- **Challenge 3: Real-Time Processing and Uncertainty Quantification** — Real-time processing and uncertainty quantification are critical for crucial rapid decision-making and fault detection. Analyzing data in real time while considering uncertainties can be demanding. Uncertainty management is more challenging but also essential.

The proposed hierarchical PHM framework addresses these challenges by providing a structured approach to modeling an APAR system.

The main contributions of this article are listed as follows:

(i) Propose a hierarchical framework for integrating PHM in active PAR (APAR). The proposed framework comprises device-level, subsystem-level, and overall system-level, and addresses the unique characteristics and complexities of APAR systems.

(ii) Formulate and analyze degradation models that capture the critical performance indicators for devices, subsystems, and the overall system.

(iii) Develop and integrate Bayesian long short-term memory (BayesLSTM) models for RUL prediction within the framework.

(iv) Perform experimental validation of the proposed BayesLSTM model within the hierarchical PHM framework.

2. RELATED WORKS

2.1. PHM Frameworks for Critical Parts/Devices

Developing PHM for complex systems with multiple subsystems and varying operational conditions is challenging. Hence, researchers have developed innovative approaches and methodologies to address some of these challenges. One such method is to use techniques to identify and perform PHM on critical parts of a system. This approach has been used in developing PHM frameworks for aircraft systems where the aero-engine [10] and landing gear [11] are identified as critical parts. Other complex systems such as ships [12] and high-speed trains [13] have also benefited from this approach. The diagnostic in these frameworks utilizes sensor data, including vibration [14], temperature [15], and other relevant parameters to monitor device health and detect anomalies or deviations from normal behavior.

2.2. PHM Frameworks for Specific Applications

PHM techniques and frameworks are often tailored to specific applications and industries, considering the unique characteristics and requirements of the targeted systems. In the aviation industry, Yang et al. [16] proposed an approach for designing a PHM framework based on the big data center. The essential technologies and applications of the proposed framework are demonstrated to serve as a reference for the aviation PHM framework research and improvement. To ensure the safety and reliability of high-speed railway systems, Feng et al. [17] developed a PHM framework with active maintenance (PHM-AM) for traction power supplies (TPSS). Similar PHM frameworks have been designed for specific industries and applications such as manufacturing [18] and unmanned aerial vehicle [19].

2.3. PHM Implementation in Radar Systems

The implementation of PHM in radar systems is relatively new and challenging due to system complexities [20]. Most researchers have identified the transmitter [21], power supply [22], cooling system [23], and other electronic parts [24, 25] as critical for diagnosis and prognosis. As an essential device of APARs, changes in the working parameters of the transmit/receive (T/R) modules directly affect the operation reliability. Wenjun et al. [26] analyzed the failure mechanism of T/R modules and suggested a method for implementing fault prognosis in APARs. To increase the accuracy of RUL prediction of T/R modules, Hou et al. [27] proposed extracting key parameters. The theoretical validity of the method is demonstrated by evaluating the fault characteristics of the T/R module. Other research studies have also proposed element failure diagnostics frameworks for APAR [28–30].

While PHM frameworks have been researched and applied in various industries, each application domain presents unique challenges and requirements. Hence, it is crucial to develop tailored frameworks that consider the specific characteristics of APAR system under consideration, such as its structure, operational conditions, and failure modes.

3. ACTIVE PHASED ARRAY RADAR CHARACTERISTICS

3.1. Configuration and Composition of APAR

An APAR essentially comprises radiating elements, T/R modules (amplifiers, phase shifters, and attenuators), beamforming network, exciter, receiver, digital signal processing (DSP), control and calibration subsystem, power supply (power converters, regulators, and distribution circuits), cooling and thermal management (heat sinks, fans, and cooling mechanisms), communication and data interface (Ethernet and serial communication), and mechanical structure (enclosure, mounting brackets, and mechanical components to ensure stability and durability). Fig. 1 illustrates the interconnections of the essential subsystems in the array.

The antenna array is the main component of the radar system and is composed of a large number of individual antenna elements arranged in a regular grid, forming a two-dimensional array. Each antenna element in the array is connected to a dedicated T/R module. These modules consist of a power amplifier for transmitting radar pulses and a low-noise amplifier for receiving the echo signals through the antenna elements. It also includes other components to process the radar signals. The T/R modules primarily contribute towards maximum radiated power and also drive the system sensitivity [31].

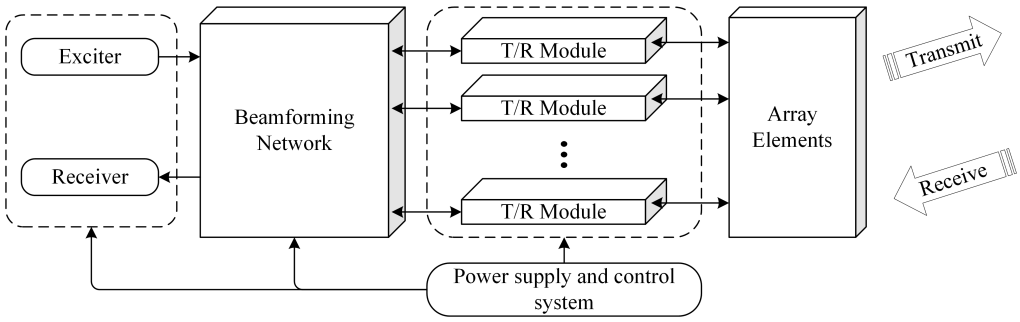

FIGURE 1. Interconnected subsystems of an active phased array system [31].

A phase shifter controls the phase of the signal transmitted or received by the antenna element. By adjusting the phase shift of each element, the radar beam can be electronically steered in a desired direction. A beamforming network combines the signals from individual antenna elements with the appropriate phase shifts to create a coherent and steerable radar beam. It controls the phase shifters of each element according to the desired beam direction. The operation of the APAR system, including beam steering, signal processing, target tracking, and other radar functions is managed by a control system. It interfaces with the beamforming network and other radar subsystems to ensure coordinated operation. The various devices and subsystems work together to form a highly flexible and electronically steerable radar beam. An APAR requires a substantial amount of power to operate efficiently. Cooling systems are essential to maintain the radar's functionality to prevent overheating [32].

The various components are categorized as follows:

(i) T/R Subsystem (radiating elements, T/R modules, and beamforming network).

(ii) Signal Processing Subsystem (DSP, control and calibration).

(iii) Support Subsystem (power supply, cooling and thermal management, communication and data interface, mechanical structure).

By categorizing the subsystems into these subgroups, a distinction is made between the major functions of core components responsible for signal transmission and reception (T/R subsystem), the processing and control elements (signal processing subsystem), and the supporting components that ensure proper power, cooling, communication, and mechanical stability (support subsystem). The degeneration of critical devices in any of these subsystems can lead to system performance degradation.

3.2. Effects of Failure on the APAR Performance

The degradation in an APAR can have several effects, impacting its performance and overall capabilities. The extent of the effect depends on the type and location of the failure. The potential effects of degradation include:

(a) *Reduced T/R Module Performance*: The failure or degradation of T/R module can decrease the overall transmitting power level. This effect can reduce detection range and diminish target tracking capabilities, especially for targets with low radar cross-section (RCS). The accuracy and precision of beam steering can also be affected if the T/R modules are not functioning optimally. This can reduce the target location estimation accuracy.

(b) *Faulty Beamforming Network*: A faulty beamforming network can introduce phase or amplitude errors across the array, which can degrade the shape of the radar beam and reduce sidelobe suppression, which impacts overall radar performance.

(c) *Faulty Devices and Components*: The failure or degradation of devices, such as phase shifters or amplifiers, can introduce signal distortions and degrade the performance integrity of the radar system. A degraded APAR will have increased sidelobe levels and become more susceptible to electronic warfare (EW) threats. Weakened performance and compromised functionality can make it easier for adversaries to disrupt or deceive the radar system, affecting situational awareness.

If degradation progresses unchecked, it can lead to an increased failure rate of T/R modules or other critical devices. As more modules fail, the effective aperture size of the APAR decreases, reducing its performance. A result of these anomalies is a decrease in the maximum detectable range given as:

$$R_{\max}(\text{New}) = R_{\max} \times \left[1 - \left(\frac{N_f}{N_T}\right)\right]^{\frac{3}{4}}, \tag{1}$$

where N_f and N_T are the failed and total numbers of elements in the array.

4. HIERARCHICAL PHM FRAMEWORK DESIGN

Developing a hierarchical PHM framework for an APAR system involves creating a structured approach to monitor, diagnose, and predict the system health at different levels.

4.1. Proposed Hierarchical PHM Structure

The proposed hierarchical PHM framework comprises system-level, subsystem-level, and device-level PHM as illustrated in

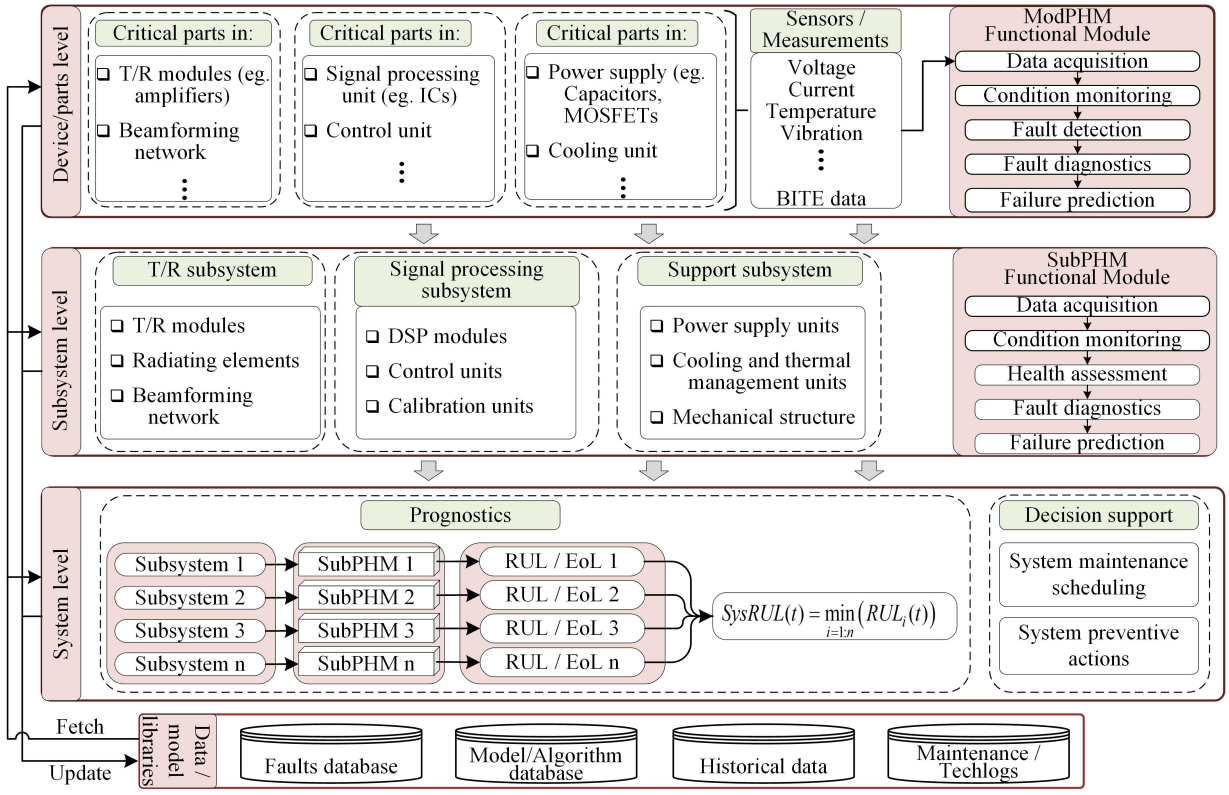

FIGURE 2. An overview of the proposed hierarchical PHM framework for APAR systems.

Fig. 2. The device-level (ModPHM) focuses on critical parts and devices such as T/R modules, amplifiers, and other critical devices. The goal is to assess their health and predict potential failures. The subsystem-level (SubPHM) aggregates the health information from multiple devices within a subsystem. The system-level (SysPHM) combines the health status of all subsystems with historical data and expert knowledge to estimate the overall system health. The various layers leverage information from the fault library, expert knowledge, historical/sensor data, and advanced DL techniques for health assessment, fault diagnosis, and failure predictions. The various layers monitor the health status of parts and devices under their jurisdiction.

• **Device-Level PHM:** At this level, the focus is on individual parts and devices. The failure mode and monitoring points of critical units are identified for sensor data acquisition. The health assessment, fault diagnosis, and failure prediction (ADP) are performed with the ModPHM model for each critical part or device. This layer forms the fundamental and crucial level of PHM implementation. The process is given in Algorithm 1.

• **Subsystem-Level PHM:** This layer focuses on subsystems and each SubPHM, corresponding to each subsystem, integrates the health information from individual devices under its jurisdiction to form a comprehensive view of a subsystem's health. Each SubPHM model performs health assessment and RUL prediction for a subsystem. This may involve combining health indicators from different devices in a meaningful way. The steps for subsystem-level PHM are given in Algorithm 2.

Algorithm 1: Device-Level PHM

Data: Device sensor data
Result: Predicted health and RUL for each device
while *Data available for devices* **do**
  Acquire data (temperature, power consumption, signal quality, etc.) from sensors;
  Preprocess the data;
  Extract health indicators;
  Detect anomalies;
  Predict RUL;
end

Algorithm 2: Subsystem-level PHM

Data: Device health and RUL information
Result: Subsystem health assessment
while *subsystems data available* **do**
  Fuse device health information;
  Assess subsystem health;
  Perform fault propagation analysis;
  Predict subsystem health and RUL;
end

The prediction outcome at this level provides actionable information regarding subsystem-level repairs or replacements.

• **System-Level PHM:** The system layer of the hierarchical PHM framework involves the aggregation of subsystem-level health predictions to provide an overall system health assessment. The system maintenance is scheduled, and various

databases and libraries are updated based on fault diagnostics and RUL predictions.

4.2. Integrated Functional Modules

The integrated functional modules incorporate techniques for executing the PHM processes in the various layers within the hierarchical framework to achieve a comprehensive system health management.

4.2.1. Data Acquisition and Preprocessing Module

Various sensors are strategically placed to collect physical parameters and other relevant APAR operating parameters. The acquired data is cleaned and conditioned to ensure accurate and reliable data for subsequent analysis. DL models can be employed for data denoising in the preprocessing module.

4.2.2. Fault Detection and Diagnosis Module

It analyzes the acquired data using various techniques to detect and identify faults or anomalies in devices or subsystems. DL algorithms can learn and classify patterns and detect anomalies in data. These models are suited for fault detection and diagnosis, and can improve accuracy and robustness.

4.2.3. RUL Estimation Module

Advanced prognostic algorithms and models estimate the degradation trends, failure probabilities, and RUL based on the available data and diagnostic information. DL-based prognostic models, such as LSTM [33], capture complex degradation patterns, and provide more accurate and reliable predictions.

4.3. Degradation Modeling and PHM Framework Development

4.3.1. Modeling Critical State Parameters

There are several factors that affect the performance of the APAR. The performance of the various subsystems is quantified by key performance indicators. In this paper, the transmitting signal power (P_t), effective radiated power (ERP), signal-to-noise ratio (SNR), noise figure (NF), frequency stability (FS), spurious free dynamic range (SFDR), transmission efficiency (η), and reflection coefficient (Γ) are selected as key performance indicators that determine the state of the APAR at time t, modeled as:

$$\begin{aligned}\boldsymbol{x}(t) \;=\; & [P_t(t), \mathrm{ERP}(t), SNR(t), NF(t), FS(t), \\ & \mathrm{SFDR}(t), \Gamma(t), \eta(t)]^T. \end{aligned} \tag{2}$$

The output power, P_t, is a combination of the power generated by each T/R module ($P_{element}$) in the array [31]. For an array with N_t elements, P_t can be expressed as:

$$P_t = P_{element} \times N_t. \tag{3}$$

The semiconductor power amplifiers used in the T/R modules are affected by internal and external conditions that lead to degradation or failure over time [34]. The ERP of the APAR is expressed as:

$$\mathrm{ERP} = P_{element} \times \left(\frac{4\pi A_{element}}{\lambda^2}\right) \times N_t^2, \tag{4}$$

where λ is the wavelength, and $A_{element}$ represents the effective aperture of an element. The loss in ERP directly quantifies the performance of APAR applications [35].

Since noise does not coherently combine, the beamformer output noise (N_{out}) is just the input noise (N_{in}), scaled by the noise factor (F). The SNR output (SNR_{out}) of the beamformer is given as:

$$\mathrm{SNR}_{out} \propto \frac{P_{element} \times (N_t - N_f)^3}{kT_oBF}, \tag{5}$$

where k, T_o, and B are the Boltzmann's constant, noise temperature, and bandwidth, respectively. N_f is the number of failed elements in the event of non-propagating elements.

NF quantifies the amount of additional noise the system introduces compared to an ideal noiseless system [36]. The cascaded noise factor in the APAR is obtained by considering the SNR at the input and outputs as follows:

$$F_{\mathrm{APAR}} = \frac{S_{in}/N_{in}}{S_{out}/N_{out}} = \left(\frac{\sum_{i=1}^{N_t} \alpha_i^2}{\left|\sum_{i=1}^{N_t} \alpha_i\right|^2}\right)(F_i), \tag{6}$$

where F_i and α_i are the noise factor and amplitude weight of the ith T/R module. $NF(dB) = 10\log(F_{\mathrm{APAR}})$.

The ability of a receiver to maintain a high SNR in the presence of spurious signals or unwanted harmonic distortions is defined by its SFDR. The minimum linear signal power should be greater than the noise floor power for increased detection probability [37]. The SFDR for an nth order output power for each T/R module is computed as:

$$\mathrm{SFDR} = 10\log_{10}\left(\frac{IPn}{kT_oBNF}\right), \tag{7}$$

where IPn represents the nth order intercept point, which measures the receiver system's linearity. It represents the input power level at which the nth order intermodulation products are equal to the desired signal power. The total SFDR is a combination of each T/R module's SFDR.

$$\mathrm{SFDR}_{combined} = \sum_{i=1} \mathrm{SFDR}_i + 10\log_{10}(N_t). \tag{8}$$

The term $10\log_{10}(N_t)$ accounts for the cascading effect assuming the spurious signals generated by each T/R module add in power, thereby increasing the overall SFDR.

The transmission efficiency (η) quantifies the efficiency with which the transmitted signal power is maintained as it passes through multiple stages in the array. There are losses or inefficiencies due to various factors, such as insertion loss,

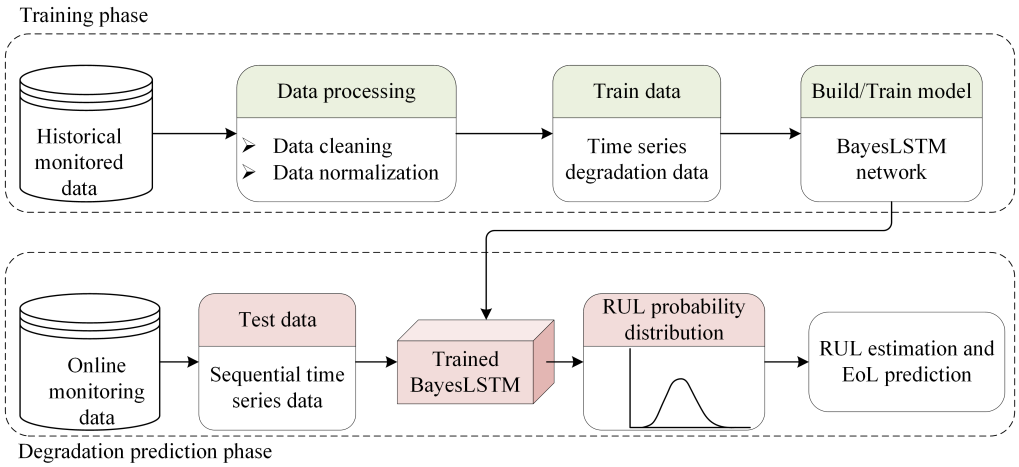

FIGURE 3. Flowchart of the proposed BayesLSTM prognostic model for RUL prediction.

impedance mismatches, power dissipation, and other associated losses [36]. Hence, the transmission efficiency of the APAR is obtained as:

$$\eta = \eta t \times \eta p \times \eta m, \tag{9}$$

where $\eta t = \prod_i^{N_t} \eta t_i$ represents the combined efficiency of T/R modules; ηp and ηm represent the power combining efficiency of the beamforming network and the matching efficiency between the T/R modules and antenna element, respectively.

The reflection coefficient is computed by considering the reflections and coupling effect that occur at each interface between the T/R modules. For each interface in a linear array with N_t elements, Γ can be calculated as:

$$\Gamma_i(\theta_0, \phi_0) = \sum_{n=1}^{N_t} C_{i,n} \frac{\alpha_n}{\alpha_i}, \tag{10}$$

where α represents the amplitude weight of each element, and $C_{i,n}$ is the effect of mutual coupling coefficients of the nth element on the ith T/R module.

4.3.2. Failure Mechanisms and Degradation Modeling

Several mechanisms degrade the physical components of the APAR system. These degradation mechanisms impact the critical state parameters. Typical performance degradation factors are:

- *Aging and Wear (A&W):* Device and components degrade due to A&W, leading to decreased performance or failure of electronic and radio frequency (RF) devices.
- *Environmental Factors (EF):* Environmental conditions such as extreme temperatures, humidity, dust, and saltwater exposure cause corrosion, insulation breakdown, and material deterioration.
- *Power Supply Issues (PS):* Unstable power supply causes voltage fluctuations or spikes that can damage or degrade electronic devices. Power surges impact components, devices, subsystems, and the overall system performance and reliability.
- *Thermal Effects (TE):* Inadequate cooling or thermal management can result in overheating of active devices leading to reduced efficiency or changes in electrical characteristics.
- *Electrical Noise (EN):* Electrical noise sources within the radar system can affect the performance of RF devices, leading to degraded signal quality, increased error rates, or reduced sensitivity.
- *Vibration and Mechanical Stress (V&S):* The APAR may be subjected to V&S due to transportation or operation in mobile platforms such as ships and aircraft. These effects can cause loosening connections, misalignment, fatigue failure, or damage to sensitive parts.

Hence, the formulation of the input vector ($\boldsymbol{u}(t)$) comprises degradation mechanisms as follows:

$$\boldsymbol{u}(t) = [A\&W(t), EF(t), PS(t), TE(t), EN(t), V\&S(t)]^T. \tag{11}$$

4.4. Prognostic Modeling within the Proposed Hierarchical PHM Framework

Predicting the RUL is the hallmark of a PHM framework. Therefore, a DL-based prognostic model with uncertainty quantification (UQ) is formulated and integrated into the hierarchical framework. Quantifying uncertainties in RUL predictions allows for more confidence and reliability of the predictive results. The confidence intervals (CIs) around the RUL predictions quantify the uncertainty associated with the predictive estimates and inform maintenance planning decision-making processes. Hence, a BayesLSTM architecture for estimating the RUL in the proposed hierarchical PHM framework is proposed. The flowchart of the BayesLSTM model is shown in Fig. 3.

Considering the first time a degrading feature hits the predefined threshold (τ), the RUL given the conditional measurement $X(t_p)$ at inspection time t_p is:

$$RUL(t_p) = \inf\{l : X(t_p + l) \geq \tau | l \geq 0, X(t_p) < \tau\}. \quad (12)$$

For N critical features, their respective RUL(t) values are denoted as $RUL_1(t), RUL_2(t), \ldots, RUL_N(t)$. The critical RUL, representing the most degrading feature, can be determined using Algorithm 3. $minRUL$ indicates the shortest remaining life among all the monitored physical and operating parameters, highlighting the most critical device in terms of reaching the set threshold. Since the RUL estimation is based on CIs, features whose RUL distributions overlap significantly can inform maintenance personnel to take informed decisions.

Algorithm 3: RUL Prediction for Multiple Critical Features

Input : $Threshold, Output_1, Output_2, \ldots, Output_N$
Output: $criticalFeature, RUL$
for $i = 1$ *to* N **do**
  if $Output_i \geq Threshold$ **then**
    $RUL_i(tp) \leftarrow$ Computed RUL of $Output_i$;
  end
  else
    $criticalFeature \leftarrow$ No variable has reached the threshold;
  end
end
$minRUL(tp) \leftarrow \min(RUL_1(tp), RUL_2(tp), \ldots, RUL_N(tp))$;
$criticalFeature \leftarrow$ Index of the minimum RUL;
return $criticalFeature, RUL(tp)$;

4.4.1. Bayesian LSTM (BayesLSTM) Modeling

A conventional LSTM cell comprises input (i_t), forget (f_t), and output (o_t) gates respectively, at time (t) expressed as [38]:

$$\begin{aligned} f_t &= \sigma\left(W_{fx}x_t + w_{fh}h_{t-1} + b_f\right) \\ i_t &= \sigma\left(W_{ix}x_t + w_{ih}h_{t-1} + b_i\right) \\ \bar{c}_t &= \tanh\left(W_{cx}x_t + w_{ch}h_{t-1} + b_c\right) \\ c_t &= f_t \cdot c_{t-1} + i_t \cdot \bar{c}_t \\ o_t &= \sigma\left(W_{ox}x_t + w_{oh}h_{t-1} + b_o\right) \\ h_t &= o_t \cdot \tanh\left(c_t\right) \end{aligned}, \quad (13)$$

where W and b are the weights and biases of the gates. $\bar{c}_t$ is the candidate cell, and x_t represents the input at time step t. The sigmoid and hyperbolic tangent activation functions are represented as σ and $tanh$, respectively. The input gate controls the flow of new information into the memory cell. The forget gate determines whose information from the previous cell state should be discarded. New values for the cell state are computed by the candidate cell. The memory cell combines the previous cell state with the new candidate values, considering the input and forget gates. Finally, the output gate controls the information from the cell to the hidden state.

The weights and biases in BayesLSTM are sampled from a probability distribution according to Eq. (14) rather than being deterministic usually associated with traditional LSTMs. The distribution of weights and biases are parameterized by the mean (μ) and standard deviation (ρ) of the input feature.

$$\begin{aligned} W_{(n)}^{(i)} &= \mathcal{N}(0,1) * \log\left(1 + \rho_{(w)}^{(i)}\right) + \mu_{(w)}^{(i)} \\ b_{(n)}^{(i)} &= \mathcal{N}(0,1) * \log\left(1 + \rho_{(b)}^{(i)}\right) + \mu_{(b)}^{(i)} \end{aligned}. \quad (14)$$

With this approach, it is possible to measure confidence and uncertainty over predictions. Given a set of data sequence $\mathbf{X} = \left\{\mathbf{x}^{(j)}\right\}_{j=1}^{p}$ and $\mathbf{Y} = \left\{\mathbf{y}^{(j)}\right\}_{j=1}^{p}$ where $x^{(j)}$ and $y^{(j)}$ denote the jth monitoring data, and p is the total number of monitoring data until the present time t_p, BayesLSTM aims to find the posterior distribution over model parameters $p(W, b|\mathbf{X}, \mathbf{Y})$.

4.4.2. Model Configuration and Performance Evaluation Metrics

The Keras hyperparameter tuner is adopted to obtain the optimum hyperparameters (number of hidden layers, number of neurons in each layer, batch size, dropout and learning rates) of the network. The search range and optimum model parameters are given in Table 1.

The dataset is reshaped using a sliding time window with optimum look back as required by the LSTM model. Threshold determination is typically based on equipment's historical records or domain-specific information. The BayesLSTM is trained with the Adam optimizer for 100 epochs using input data of various sample sizes. The prediction performance is evaluated based on the absolute error (AE), root mean square error (RMSE), and relative accuracy (RA) between the actual and predicted values.

5. EXPERIMENTS

Several experiments are performed to predict the degradation trend and estimate the RUL of a critical performance feature. The experiments are conducted using Keras framework and Python 3.7, and executed on a Windows OS platform with 16 GB RAM and a 4GB NVIDIA GeForce RTX 3050 GPU.

5.1. Dataset Generation and Description

Due to the lack of publicly available radar performance data, experimental data is generated to represent a degrading subsystem feature to evaluate the proposed DL-based prognostic model. The degradation data is generated using PrognosEase [39], an open-source data generator that generates deterioration measures based on user-specified characteristics to simulate real-world situations. It is assumed that the degradation of devices in the T/R subsystem degrades its transmitted power over time as shown in Fig. 4. The monitoring point has 500 historical data points. The vertical axis represents the data value of the monitoring sensor, and the horizontal axis represents the time step of the sampling point. The time-series sensor data is first denoised using the moving average filter.

The BayesLSTM is trained with $t_p = 60$, 70, 80, and 90% of the data, and its performance is evaluated on the remaining 40, 30, 20, and 10%, respectively. A soft threshold value of 5.54 kW is set for the experiment.

TABLE 1. Search range and optimum model hyperparameters.

	Hyperparameters				
	# of layers	# of units	batch size	dropout rate	learning rate
Range *	[1, 3, 1]	[20, 100, 20]	[8, 32, 8]	[0.0, 0.6, 0.2]	[0.01, 0.1, 0.01]
Optimal value	1	60	8	0.0	0.01

* [a,b,c] denotes the hyperparameter search space ranging from minimum (a) to maximum (b) with a step size (c).

TABLE 2. Prediction performance at different prediction times.

Subsystem	t_p	Actual RUL	Pred EoL	Pred RUL	AE	RMSE	RA (%)
	300	190	468	168	22	0.03358	88.42
T/R	350	140	495	145	5	0.02180	96.43
subsystem	400	90	493	93	3	0.02167	96.67
	450	40	491	41	1	0.01526	97.5

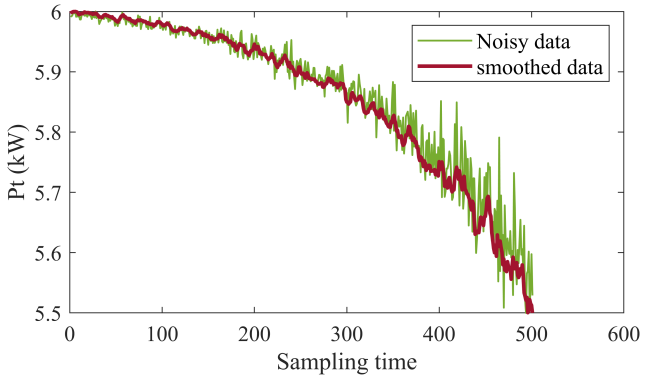

FIGURE 4. T/R subsystem degradation data before and after denoising.

5.2. Experimental Results Analysis

5.2.1. RUL Estimation

In this experiment, the BayesLSTM output is modeled as a Normal distribution, with learnable mean and variance parameters. The mean of the estimated RUL for different t_p is presented in Table 2. The various performance results are also included in the table for analysis.

The predictions are generated for the degradation state at each future time by training the probabilistic BayesLSTM to account for uncertainty. These experiments produced distribution of predictions, and the average value is computed for each future time. Fig. 5 shows the average degradation prediction along with a 95% confidence interval for different prediction times. The 95% confidence interval encompasses all the future predictions, indicating that our degradation prediction effectively captures uncertainty and accurately represents the actual trajectory.

It can also be observed from Figs. 6(c) and 6(d) that at the initial prediction stage, there is a large deviation between the predicted RUL and the actual RUL. Because of the lack of degradation information, the modeling errors are large at the beginning, but as more data becomes available, the deviation and uncertainty from modeling errors decreases gradually as indicated in Figs. 6(a) and 6(b). Table 2 also highlights the prediction performance at four different t_p. For each t_p, the table provides the actual RUL (Actual RUL), predicted EoL (Pred EoL), and predicted RUL (Pred RUL). The AE and RA characterize the deviation between the predicted RUL and true RUL, while RMSE quantifies both the deviation and uncertainty of the RUL prediction.

It is worth pointing out that the lesser the AE and RMSE are, the better the performance is in RUL prediction. Such a relationship is just the opposite for RA. At a $t_p = 300$, the mean predicted RUL is 168, whereas the actual RUL is 190, resulting in an AE of 22. This value is the highest observed even though RA is around 88%. However, the AEs for the other prediction start times decrease when more sample data are available for training the model. It can be observed that the AEs for $t_p = 350$, 400, and 450 are less or equal to five, and the AE for $t_p = 450$ is less than one. Similarly, all of the RAs at various prediction times are large enough, ranging from 88.42% to 97.5%. Moreover, the various prediction RMSEs are relatively low with the highest being 0.03358 and the lowest 0.01526.

Therefore, the proposed method can not only hold the high accuracy of the RUL prediction for a degrading subsystem but also express the uncertainty of the RUL prediction which is beneficial.

5.2.2. Uncertainty Expression of Prediction Results

The proposed BayesLSTM algorithm is used to make degradation predictions, and the future estimated state is obtained with uncertainty expressions. In this paper, uncertainty analysis is carried out at different prediction times as shown in Table 2. The relationship between estimated values at different EoL predictions with 95% CI is given in Table 3. It can be concluded with 95% confidence that the true and expected mean prediction results lie within the CI. The results show that the proposed degradation trend prediction method has high accuracy in quantifying the model and data uncertainties.

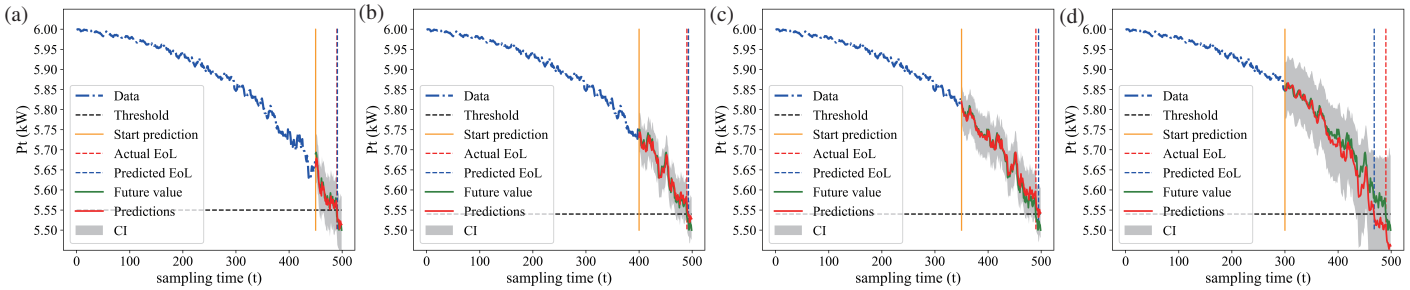

FIGURE 5. Average prediction results with 95% CI. (a) $t_p = 450$; (b) $t_p = 400$; (c) $t_p = 350$; (d) $t_p = 300$.

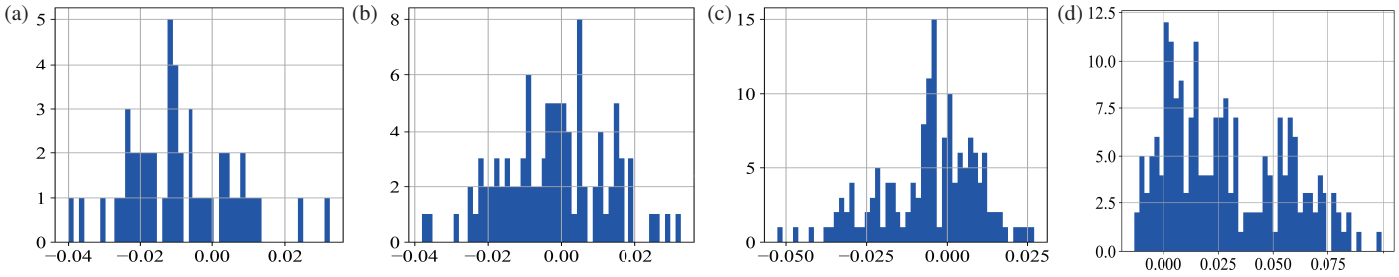

FIGURE 6. Prediction error distribution. (a) $t_p = 450$; (b) $t_p = 400$; (c) $t_p = 350$; (d) $t_p = 300$.

TABLE 3. Uncertainty quantification for different prediction start times.

t_p	Actual EoL	Predicted EoL	Predicted Power (kW) @EoL	95% CI
60	490	468	5.5357	[5.3392, 5.6839]
70	490	495	5.5367	[5.3525, 5.6729]
80	490	493	5.5368	[5.4584, 5.6153]
90	490	491	5.5231	[5.4412, 5.6050]

The predicted EoL and RUL for the T/R subsystem provide an estimate of when it is likely to fail. This information can be used to schedule maintenance activities proactively, ensuring that necessary repairs or replacements are carried out before a failure occurs. It allows maintenance teams to prioritize maintenance actions based on the urgency of the predicted failures. Components with a shorter predicted RUL can be prioritized for maintenance or replacement, while those with a longer predicted RUL can be scheduled for maintenance at a later date. This enables effective resource allocation and helps in making informed decisions regarding maintenance scheduling.

6. CONCLUSION

This paper advances PHM techniques by proposing a hierarchical PHM framework tailored for APAR systems to enhance health monitoring and RUL prediction. A structured approach that leverages the advantages of hierarchical modeling and facilitates the integration of diverse models is presented. The proposed framework offers a comprehensive approach to addressing the challenges of integrating PHM in APAR systems, paving the way for improved operational efficiency. By integrating DL models into the proposed framework, the approach harnesses the power of data-driven modeling while reducing the impact of prediction uncertainties.

A probabilistic approach to prognostic modeling and uncertainty quantification using BayesLSTM models integrated within the proposed framework is demonstrated. The model's prediction results are evaluated with data samples of different lengths. The prognostic results based on RUL predictions are high with RA between 88.42% and 97.5%. This highlights the effectiveness of the proposed prognostic model in estimating the RUL with confidence bounds.

ACKNOWLEDGEMENT

This work was supported by the National Natural Science Foundation of China (Grant No. 42027805).

REFERENCES

[1] Talisa, S. H., K. W. O'Haver, T. M. Comberiate, M. D. Sharp, and O. F. Somerlock, "Benefits of digital phased array radars," *Proceedings of the IEEE*, Vol. 104, No. 3, 530–543, 2016.

[2] Mailloux, R. J., *Phased Array Antenna Handbook*, Artech House, 2017.

[3] Kulevome, D. K. B., W. Hong, X. Wang, B. M. Cobbinah, B. L. Y. Agbley, and Q. Safder, "System diagnosis frame-

work for sustaining the operational fidelity of a radar system," *2021 18th International Computer Conference on Wavelet Active Media Technology and Information Processing (ICCWAMTIP)*, 640–644, 2021.

[4] Kim, N. H., D. An, and J. H. Choi, *Prognostics and Health Management of Engineering Systems*, Springer International Publishing, Switzerland, 2017.

[5] Xu, J., Y. Wang, and L. Xu, "PHM-oriented integrated fusion prognostics for aircraft engines based on sensor data," *IEEE Sensors Journal*, Vol. 14, No. 4, 1124–1132, 2013.

[6] Nguyen, D., et al., "A review: Prognostics and health management in automotive and aerospace," *International Journal of Prognostics and Health Management*, Vol. 10, No. 2, 35, 2019.

[7] Agyemang, I. O., X. Zhang, I. Adjei-Mensah, J. R. Arhin, and E. Agyei, "Lightweight real-time detection of components via a micro aerial vehicle with domain randomization towards structural health monitoring," *Periodica Polytechnica Civil Engineering*, Vol. 66, No. 2, 516–531, 2022.

[8] Celaya, J. R., C. S. Kulkarni, G. Biswas, and K. Goebel, "Towards a model-based prognostics methodology for electrolytic capacitors: A case study based on electrical overstress accelerated aging," *International Journal of Prognostics and Health Management*, Vol. 3, No. 2, 2020.

[9] Niu, G., *Data-Driven Technology for Engineering Systems Health Management: Design Approach, Feature Construction, Fault Diagnosis, Prognosis, Fusion and Decisions*, Springer, Singapore, 2017.

[10] Wang, C., N. Lu, Y. Cheng, and B. Jiang, "A data-driven aero-engine degradation prognostic strategy," IEEE Transactions on Cybernetics, Vol. 51, No. 3, 1531–1541, 2019.

[11] Hsu, T. H., Y. J. Chang, H. K. Hsu, T. T. Chen, and P. W. Hwang, "Predicting the remaining useful life of landing gear with prognostics and health management (PHM)," *Aerospace*, Vol. 9, No. 8, 462, 2022.

[12] Zhang, P., et al., "Marine systems and equipment prognostics and health management: a systematic review from health condition monitoring to maintenance strategy," *Machines*, Vol. 10, No. 2, 72, 2022.

[13] Chi, Z., J. Lin, R. Chen, and S. Huang, "Data-driven approach to study the polygonization of high-speed railway train wheel-sets using field data of china's HSR train," *Measurement*, Vol. 149, 107022, 2020.

[14] Kulevome, D. B. K., H. Wang, and X. Wang, "Deep neural network based classification of rolling element bearings and health degradation through comprehensive vibration signal analysis," *Journal of Systems Engineering and Electronics*, Vol. 33, No. 1, 233–246, 2022.

[15] Zhang, D., C. Cadet, N. Yousfi-Steiner, F. Druart, and C. Berenguer, "PHM-oriented degradation indicators for batteries and fuel cells," *Fuel Cells*, Vol. 17, No. 2, 268–276, 2017.

[16] Yang, L., J. Wang, and G. Zhang, "Aviation PHM system research framework based on PHM big data center," *2016 IEEE International Conference on Prognostics and Health Management (ICPHM)*, 1–5, 2016.

[17] Feng, D., S. Lin, Z. He, and X. Sun, "A technical framework of PHM and active maintenance for modern high-speed railway traction power supply systems," *International Journal of Rail Transportation*, Vol. 5, No. 3, 145–169, 2017.

[18] Fumagalli, L., et al., "Framework for PHM in the smart manufacturing context: integration of different approaches," *MFPT 2017 Annual Conference: 50 Years of Failure Prevention Technology Innovation*, 1–11, 2017.

[19] Dingeldein, L., "Simulation framework for real-time PHM applications in a system-of-systems environment," *Aerospace*, Vol. 10, No. 1, 58, 2023.

[20] Lyu, Y., Z. Pang, C. Zhou, and P. Zhao, "Prognostics and health management technology for radar system," *MATEC Web of Conferences*, Vol. 309, 04009, 2020.

[21] Zhai, Y. and S. Fang, "A degradation fault prognostic method of radar transmitter combining multivariate long short-term memory network and multivariate Gaussian distribution," *IEEE Access* Vol. 8, 199781–199791, 2020.

[22] Li, Q., Y. Lv, Z. Chuang, and H. Qu, "Research on power supply performance degradation based on neighborhood rough set and multiple linear regression," *2019 Prognostics and System Health Management Conference (PHM-Qingdao)*, 1–7, 2019.

[23] Wang, C., N. Lu, Y. Chen, and H. Yu, "A data-driven fault detection method for radar cooling system," *2021 CAA Symposium on Fault Detection, Supervision, and Safety for Technical Processes (SAFEPROCESS)*, 1–5, 2021.

[24] Dai, P. and W. Yu, "Overview of radar digital circuit fault detection technology," *2020 IEEE 5th Information Technology and Mechatronics Engineering Conference (ITOEC)*, 88–92, 2020.

[25] Kulevome, D. B. K., H. Wang, and X. Wang, "A bidirectional LSTM-based prognostication of electrolytic capacitor," *Progress In Electromagnetics Research C*, Vol. 109, 139–152, 2021.

[26] Wenjun, G., S. Bin, and Z. Yuanzhu, "Fault prognosis of transmit-receive modules for active phased array radar," *Global Reliability and Prognostics and Health Management (PHM-Nanjing)*, 1–6, 2021.

[27] Hou, X., J. Yang, B. Deng, L. Xia, Y. Zhang, and Z. Zhang, "A key lifetime parameters extraction method for T/R module based on association rule," *2018 International Conference on Sensing, Diagnostics, Prognostics, and Control (SDPC)*, 165–170, 2018.

[28] Nielsen, M. H., M. H. Jespersen, and M. Shen, "Remote diagnosis of fault element in active phased arrays using deep neural network," *27th Telecommunications Forum (TELFOR)*, 1–4, 2019.

[29] De Lange, L., "Machine learning for antenna array failure analysis," Ph.D. Thesis, Stellenbosch University, Stellenbosch, 2020.

[30] Kulevome, D. K. B., H. Wang, X. Wang, R. Kumar, and B. Cobbinah, "Phased array antenna diagnosis from amplitude-only data using parallel deep learning models," *Journal of Applied Remote Sensing*, Vol. 17, No. 1, 017502, 2023.

[31] Brown, A. D., *Active Electronically Scanned Arrays: Fundamentals and Applications*, John Wiley & Sons, New Jersey, 2021.

[32] Park, J. S., D. J. Shin, S. H. Yim, and S. H. Kim, "Evaluate the cooling performance of transmit/receive module cooling system in active electronically scanned array radar," *Electronics*, Vol. 10, No. 9, 1044, 2021.

[33] Zheng, S., K. Ristovski, A. Farahat, and C. Gupta, "Long short-term memory network for remaining useful life estimation," *2017 IEEE International Conference on Prognostics and Health Management (ICPHM)*, 88–95, 2017.

[34] Raffo, A., G. Avolio, V. Vadala, G. Bosi, G. Vannini, and D. Schreurs, "Assessing GaN FET performance degradation in power amplifiers for pulsed radar systems," *IEEE Microwave and Wireless Components Letters*, Vol. 28, No. 11, 1035–1037, 2018.

[35] Keizer, W. P., "Element failure correction for a large monopulse phased array antenna with active amplitude weighting," *IEEE Transactions on Antennas and Propagation*, Vol. 55, No. 8, 2211–2218, 2007.

[36] Mahafza, B. R., *Introduction to Radar Analysis*, CRC Press, 2017.

[37] Rohde, U. L. and H. Zahnd, *Software Defined Radio, Receiver and Transmitter Analysis. Fundamentals of RF and Microwave Techniques and Technologies*, Springer, 2023.

[38] Yu, Y., X. Si, C. Hu, and J. Zhang, "A review of recurrent neural networks:LSTM cells and network architectures, *Neural Computation*, Vol. 31, No. 7, 1235–1270, 2019.

[39] Berghout, T., M. D. Mouss, L. H. Mouss, and M. Benbouzid, "ProgNet: A transferable deep network for aircraft engine damage propagation prognosis under real flight conditions," *Aerospace*, Vol. 10, No. 1, 10, 2022.